

PAPER • OPEN ACCESS

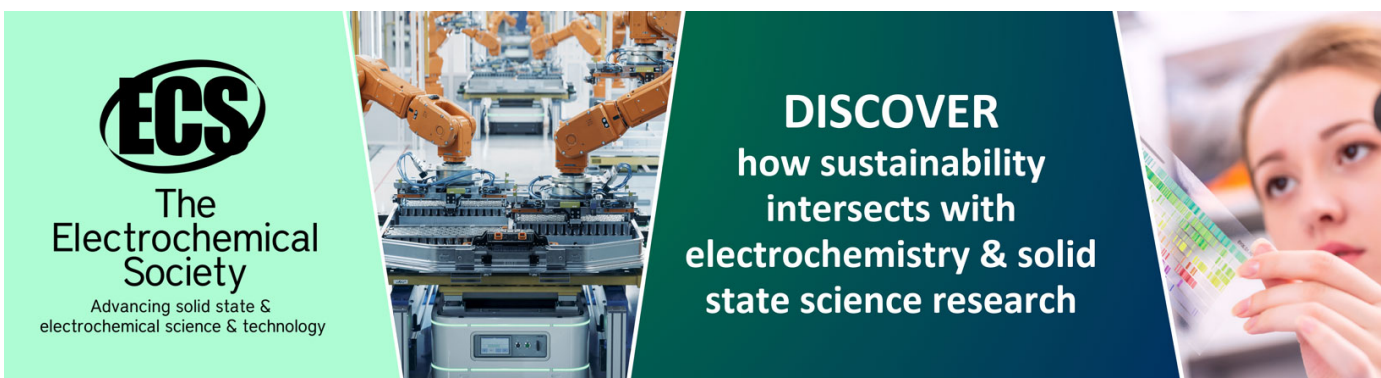
Transmission and Frequency Characteristics of Stress Waves through the Cemented Joint of Rock Mass

To cite this article: Chunyang Cui *et al* 2020 *IOP Conf. Ser.: Earth Environ. Sci.* **570** 032014

View the [article online](#) for updates and enhancements.

You may also like

- [Mesoscale strain and damage sensing in nanocomposite bonded energetic materials under low velocity impact with frictional heating via peridynamics](#)
Krishna Kiran Talamadupula, Stefan J Povolny, Naveen Prakash *et al.*
- [PZT sensor array for local and distributed measurements of localized cracking in concrete](#)
Arun Narayanan, Amarteja Kocherla and Kolluru V L Subramaniam
- [Some fundamental problems concerning the measurement accuracy of the Hopkinson tension bar technique](#)
Yinggang Miao, Bing Du, Chenbo Ma *et al.*



ECS
The
Electrochemical
Society
Advancing solid state &
electrochemical science & technology

DISCOVER
how sustainability
intersects with
electrochemistry & solid
state science research

Transmission and Frequency Characteristics of Stress Waves through the Cemented Joint of Rock Mass

Chunyang CUI¹, Qingxin QI¹, Haitao LI¹, and Zhongxue SUN²

¹Deep Mining and Rockburst Research Institute, China Coal Research Institute, Beijing, China

²Mine Safety Technology Branch of China Coal Research Institute, Beijing, China

E-mail: cuicy10_thu@163.com

Abstract. During the process of rock dynamic fracture, the rock mass releases a huge amount of fracture energy, which primarily transforms into a strong stress wave; the stress wave can cause serious damage to the neighboring zones when passing through the structural rock medium. In this study, the transmission and frequency features of the stress wave through cemented joints are investigated. The polyurethane (PU) is chosen as the cementing material to glue the cut faces of the rock sample. The bonding stiffness of joints is adjusted by the mixing proportion of the polyurethane diluent. By conducting the Split Hopkinson Pressure Bar (SHPB) test, the effect of the stiffness and thickness of the PU adhesive layer is studied by monitoring the coefficients of reflection, transmission, and dissipation, as well as the frequency components. The testing results indicate that the transmission effect increases significantly, whereas the dissipation decreases with the growth of the bonding stiffness. The increasing impact energy results in a higher degree of body fracture and crack density. The low-pass filtering (LPF) effect of the stress wave is observed evidently in low bonding stiffness.

1. Introduction

Some of the rock and coal burst hazards are triggered by the external dynamic loads, which include the natural fracture of neighboring faults, the shock wave from the blasting mining, and even the artificial disturbance from excavation. Previous studies have shown that the energy and frequency features obtained from the initial impact location and the secondary failure location vary significantly [1-3], thereby indicating that the structural rock-coal medium plays an important role in wave filtering and attenuating. In fact, the discontinuity nature of the rock and coal material, such as faults, fissuring, cracks, and artificial surfaces, primarily determines the change of wave energy and frequency [1]. L.F. Fan et al. used the discontinuous deformation analysis (DDA) approach to reveal the effect of joint stiffness and wave impedance on the wave propagation. The numerical results show that the joint stiffness is positively correlated with the stress and energy transmission ratio, and the low-frequency components are more adaptive to the weak joints [4]. Wenjun Gong et al. used a large-scale DDA rock-joint model to study the mechanical features of P-wave propagation across rock fractures. The results reveal that a higher joint stiffness can raise the energy transmission coefficient, and the LPF effect is observed evidently in both theoretical and DDA results [5].

However, most of the discontinuities mentioned above are frictional and cohesionless, which is insufficient to cover the entire natural cases. For instance, the argillaceous fillings in the cracks can turn into a form of an adhesive layer using the physicochemical and biochemical procedure, such as a siliceous and calcareous adhesive layer, salt precipitation, or biological cementation. The adhesive



layer provides additional tensile and shearing strength to the discontinuities, which leads to a different dynamic response when the stress wave passes through. Chengxue She et al. presented a compressive shear experiment of cement-filled hard rock joint. Based on the experimental strength-strain lines of joints with and without cement, it can be concluded that the cement matrix increased the peak strength and created a softening period after the peak. Additionally, the cohesive strength increased evidently, while the internal friction angle decreased under the cementing condition [6]. Hao Ma et al. conducted the same test on the cement-filled rock joint, in which the water-cement ratio controlled the cementing strength. The experimental result indicated that the peak and residual strength of the cemented joint presented a significantly positive correlation with the material strength of cement [7]. Diyuan Li et al. tested the dynamic behavior of the cemented rock joint. This indicated that the transmission coefficient of the stress wave when passing through a slant joint was only 40%–50%, which was confirmed using the SHPB impact test [8].

As discussed above, the cemented rock joint exists widely in nature and plays an important role in energy propagation, while the corresponding experimental research has just begun. Hence, the present paper focuses on the dynamic response of the cemented joint by conducting the SHPB experiment. The orthogonal experiments are designed to study the influence of the stiffness and thickness of the adhesive layer. To reproduce the natural adhesive layer with different hardness, the polyurethane is chosen as the ideal adhesive material whose Young's modulus or Shore's hardness is adjusted by mixing specific proportions of polyurethane diluent. The energy and time-frequency properties of the reflected and transmitted stress wave are studied. Finally, experimental analysis on different layer stiffness and thickness is systematically concluded.

2. SHPB Experimental System and Specimen Preparation

The testing equipment of the rock dynamic properties includes the cyclic loading triaxial testing machine, the spring drop hammer impact machine, and the SHPB impact system. To investigate the dynamic mechanism of the stress wave before and after the joint face, the testing system is required to reproduce the real wave transmission process under laboratory conditions. For this reason, the total length of the wave propagation path should be long enough, and the damping device at the end is required to avoid the wave distortion induced by the cyclic oscillation of the excess energy. The present paper chose the SHPB impact system that met the mentioned requirement to study the dynamic response of the cemented rock joints.

2.1. SHPB Impact Testing System

The SHPB system in the present paper is employed from the Key Laboratory of Shale Gas and Geoenvironment, Institute of Geology and Geophysics, Chinese Academy of Sciences, Beijing, China. The system can conduct both the dynamic compression and dynamic split tests of the Brazilian disc [9]. Figure 1 shows a photo of the equipment. Figure 2 represents the corresponding two-dimensional (2D) structure drawing. The system mainly consists of a steel frame, a gas gun, a striker bar, an incident bar, a testing specimen, a transmitted bar, and sensors. The striker, in addition to the incident and transmitted bars, is arranged along the same axis with a diameter of 50mm, which could move freely through the holes on the steel frame. The initial velocity v_0 of the striker could reach 40m/s and the impact-induced strain rate ranges from 50/s to 300/s. Moreover, the waveform shaper and wedge-shaped striker are used to generate a half-sine stress wave, as shown in Figure 5.



Figure 1. Photo of the SHPB impact system

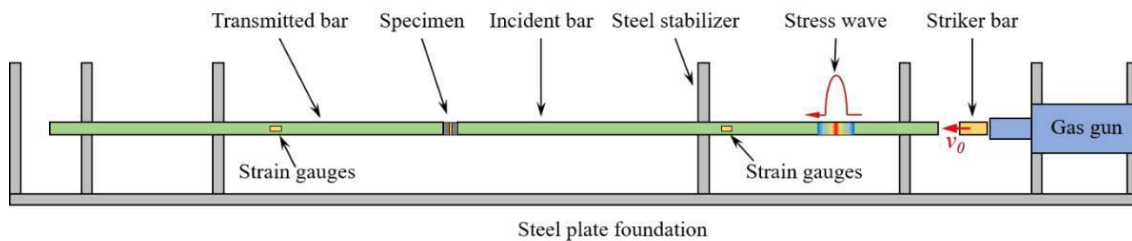


Figure 2. Schematic view of the SHPB system

2.2. Testing Specimens and Cementing Method

The fine sandstone and polyurethane are employed to form the testing specimen with a cemented joint. The polyurethane (PU) adhesive layer belongs to a high-molecular polyester compound, which has a nature of excellent chemical stability, mechanical property, and adjustability. Before the curing process, the PU remains in liquid form, which provides convenience for the pouring and curing process. Once the PU curing agent is added, the adhesive material will solidify and form stable strength within 7–10 days (depending on the mixing proportion) at room temperature. Furthermore, by mixing with varying proportions of the PU diluent, the Shore's hardness could be artificially adjusted between A30 and D85. This special process enables controlling the Shore's hardness of the adhesive layer as well as the joint stiffness from a jelly state to a quite rigid state.

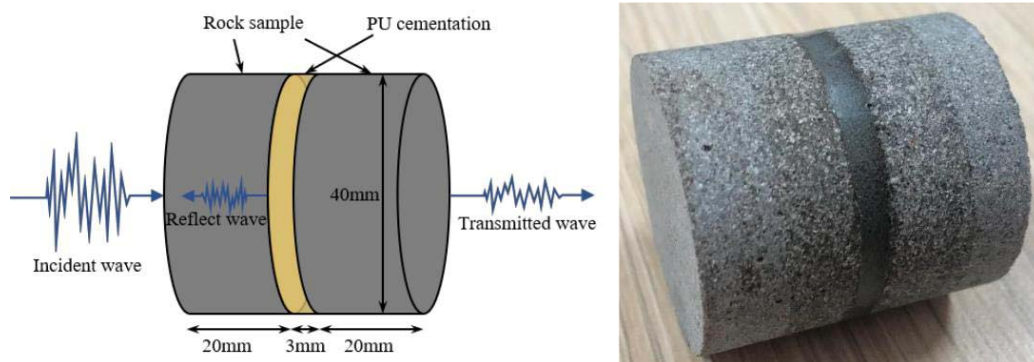


Figure 3. Diagrammatic drawing and photo of the cemented specimen

Figure 3 presents a diagrammatic drawing of the cemented specimen and corresponding stress wave. The shape of the specimen is a cylinder with a diameter of 40mm. Furthermore, based on the

experimental program in Table 2, the experiment provides three levels of the adhesive layer thickness, namely, 1mm, 3mm, and 5mm. For this reason, the corresponding height of the specimens is 41mm, 43mm, and 45mm, respectively. The rock samples were cut by an annular cutting machine and then sliced with a height of 20mm. To form the adhesive layer between two rock samples, the rock samples were first fixed with a gap of 1mm, 3mm, and 5mm and then wrapped by tapes. The PU was then poured into the gap and cured at room temperature.

The PU adhesive layer required a polyisocyanate curing agent to solidify and form strength, which was distinguished by components A and B. Different mixing proportions of A:B helped determine the hardness or modulus of the final adhesive layer. The initial setting time was 30–45 min and the final setting time was 7–10 days at room temperature. For this reason, all of the components were weighed and mixed for 10 min and poured into the joint space and then cured for 10 days before the test.

3. Experimental Study on the Dynamic Behavior of Cemented Joints

The focus of the present research is on the dynamic response and transmitting features when the high strain-rate stress wave passes through the cemented joints. The independent variables include the modulus and thickness of the PU adhesive layer. The dependent variables include the coefficients of reflection, transmission, dissipation, and the frequency spectrum.

3.1. Mechanical Parameter Experiments

Before the SHPB test, the elastic modulus of the pure PU mixture was measured by the uniaxial compression test, in which the loading rate was set as 0.1mm/min. In this study, there are five grades of layer hardness from A30 to D85 and three grades of layer thickness, which are 1mm, 3mm, and 5mm. Table 1 lists the corresponding modulus of different mixing proportions.

Table 1. Modulus of different PU mixtures

Material number	Mixing proportion A:B	Modulus (MPa)
1	1:1	0.57
2	1.5:1	7.37
3	2:1	19.71
4	2.8:1	53.28
5	3.5:1	124.08

3.2. SHPB Experiment

The numbered specimens were slightly clamped by the incident and transmitted steel bars, as shown in Figure 4. The planes of each sample were polished to keep them parallel; otherwise, the rock-steel contact could turn into a point-face contact instead of a face-face contact. According to the testing results, the point-face contact generated strong stress concentration to the fracture mode where the crack density was much higher than the non-contact region.



Figure 4. Detailed photo of the specimen and steel bars

Table 2 lists the testing sequence of different modulus and thickness values of the adhesive layer. In the experiment, the specimens kept intact at an air pressure of 0.16MPa, slightly cracked at 0.20MPa, and totally fractured at 0.26MPa. The residual specimens were collected for the analysis of crack propagation and fracture mode.

Table 2. Experimental program

Experiment serial number	Material number	Thickness (mm)
1-1 1-2	1	3.0
2-1 2-2	2	3.0
3-1 3-2	3	3.0
4-1 4-2	4	3.0
5-1 5-2	5	3.0
3-3	3	1.0
3-4	3	5.0

4. Experimental Results and Analysis

4.1. Effect of the Modulus of Cemented Joint

Figure 5 presents the incident and transmitted waveforms of the fractured samples under the air pressure of 0.26MPa. According to Table 1, the modulus of the cemented joint increases from 0.57MPa (A:B=1:1) to 124.08MPa (A:B=3.5:1), which promotes the wave transmission and depresses the reflection and the LPF effect. To analyze the waveform quantitatively, the dimensionless coefficients of reflection A_r , transmission A_t , and dissipation A_d are defined with the energy form.

Equation 1: The elastic energy of the incident wave.
$$= \int^2 2 () \quad (1)$$

Equation 2: The elastic energy of the transmitted wave.
$$\frac{\Gamma}{\Gamma} = \int^2 2 () \quad (2)$$

Equation 3: The elastic energy of the reflected wave.
$$= \frac{1}{2} \int^2 2 () \quad (3)$$

Equation 4: The dissipation energy.
$$= \frac{1}{2} \int^2 2 () \quad (4)$$

Equation 5: The coefficient of transmission.
$$= \frac{1}{2} \int^2 2 () \quad (5)$$

Equation 6: The coefficient of reflection.
$$= \frac{1}{2} \int^2 2 () \quad (6)$$

Equation 7: The coefficient of dissipation.
$$= \frac{1}{2} \int^2 2 () \quad (7)$$

- A_e = sectional area of the steel bar
- $\rho e C_e$ = wave impedance of the steel bar

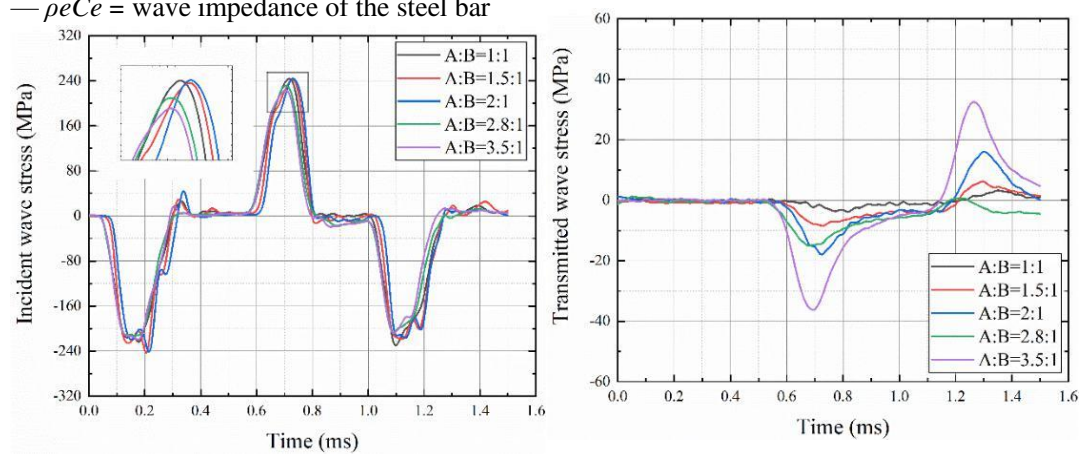


Figure 5. The incident and transmitted waveforms of cemented joints with various moduli

Based on the calculation results listed in Table 3, it can be seen that the moduli of the cemented joints significantly affect the stress wave propagation and frequency property. The energy transmission coefficient A_t increases significantly when the modulus of the adhesive layer increases, indicating that a soft and weak cemented joint can protect the structures behind the layer by suppressing the transmission of the wave energy. Essentially, the photos of the residual samples provide sufficient evidence to confirm this protective effect, as shown in Figure 6. As the adhesive layer becomes harder, the number of the post-layered macrocracks increases significantly, which is induced by the growth of the transmitted impact energy. Furthermore, the reflection coefficient A_r is roughly inversely proportional to the layer modulus, which seems to have a seesaw effect between the transmission and reflection. To quantify the LPF effect of the PU adhesive layer, the travel time reciprocal of the first transmitted pulse was calculated in Table 3. It can be seen that the soft layer has a promising capacity to keep out the high-frequency component of the stress wave.

Table 3. The energy coefficients and frequency of different adhesive layer materials

Material number	Modulus (MPa)	Reflection coefficient A_r	Transmission coefficient A_t	Dissipation coefficient A_d	Frequency (Hz)
1	0.57	96.5%	0.03%	3.5%	1408.4
2	7.37	88.6%	0.23%	11.1%	1538.4
3	19.71	88.4%	0.67%	10.9%	1694.9
4	53.28	93.0%	0.79%	6.2%	1785.7
5	124.08	83.7%	2.94%	13.3%	1851.8

Figure 6 presents the crack path and fracture mode of the residual samples. In addition to the above-mentioned macrocracks on the transmitted face, the connectivity of the spalling cracks on the lateral has evident relations with the layer moduli as well. As shown in the middle column of Figure 6, the incident cracks have no connectivity with the transmitted cracks in numbers 1 and 2, while they tend to connect near the layer surface in numbers 4 and 5. Therefore, it can be seen that a soft and weak adhesive layer could have the nature of preventing crack penetration.

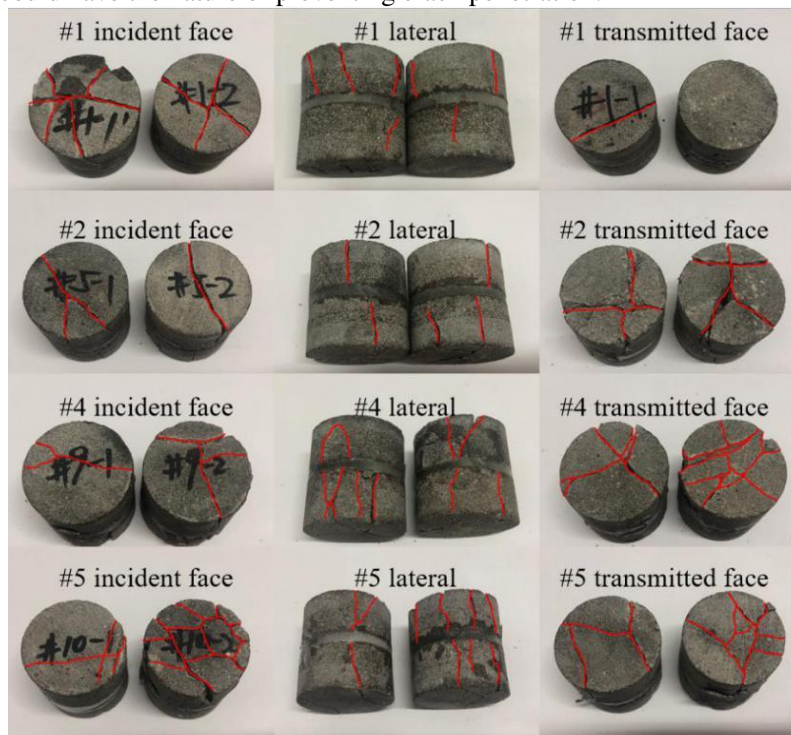


Figure 6. The fracture modes of the cemented specimen with different PU materials

4.2. Effect of the Thickness of Cemented Joint

Three cemented specimens with the adhesive layer thickness of 1mm, 3mm, and 5mm were tested under the air pressure of 0.20MPa, as shown in Figure 7. Table 4 demonstrates the corresponding energy coefficients and frequencies.

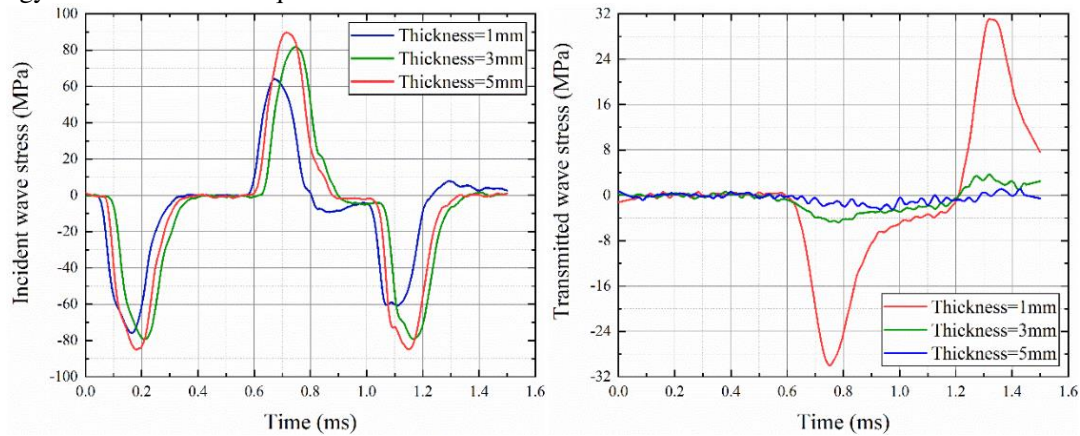


Figure 7. The incident and transmitted waveforms of cemented joints of different layer thickness

Table 4. The energy coefficients and frequency of different layer thickness

Adhesive layer thickness (mm)	Reflection coefficient A_r	Transmission coefficient A_t	Dissipation coefficient A_d	Frequency (Hz)
1	65.7%	18.4%	15.9%	1845.0
3	78.2%	0.7%	21.1%	1634.0
5	97.7%	0.2%	2.1%	1424.5

It can be concluded from Table 4 that the adhesive layer of 5mm thickness can prevent the wave energy transmission and promote the reflection effect significantly. Moreover, this layer thickness has the nature of the LPF effect that is similar to the soft and weak layer. The incident cracks in Figure 8 become longer and wider when the layer reflects more impact energy to the incident end. Furthermore, a similar phenomenon can be observed from the transmitted end. The transmitted rock body with a 5mm layer even stays intact after the test, while the body with a 1mm layer has serious spalling damage. In addition, the crack penetration is stopped by the layer of 3mm and 5mm, as shown in the middle row of Figure 8.

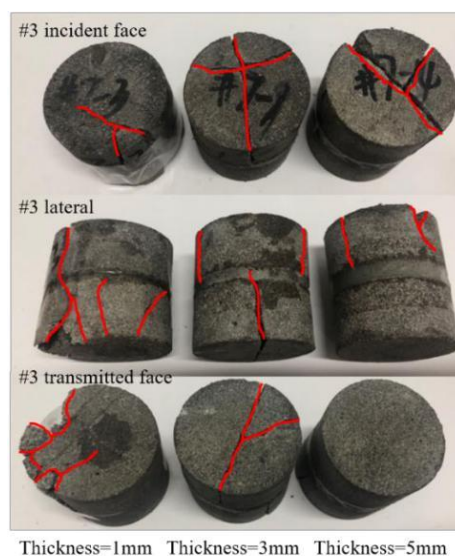


Figure 8. The fracture modes and crack penetration of the specimen with different layer thickness

5. Conclusions

The wave transmission, fracture mode, and crack penetration features of the adhesive layer were studied using the SHPB impact system. Based on the testing results, the following conclusions can be drawn:

The soft and weak adhesive layer has the nature of isolating energy transmission and crack penetration. When the modulus of the adhesive layer decreases from 124MPa to 0.57MPa, the proportion of the energy transmission decreases by 99%, and the energy reflection increases by 15%. Meanwhile, the frequency of the transmitted pulse decreases by 24%, which is recognized as the LPF effect.

The thickness of the adhesive layer has a similar effect on the above-mentioned variables. A thick layer can prevent the impact energy and cracks from passing through the joint efficiently and provides a promising LPF effect.

Based on the fracture modes of the residual specimens, it can be concluded that higher energy accumulation at one end will cause a higher degree of crushing and spalling failure at the same end. The reflected energy has a seesaw effect with the transmitted energy.

References

- [1] GOU Yonggang, SHI Xiuzhi, QIU Xianyang, et al, 2019. Propagation characteristics of blast-induced vibration in parallel jointed rock mass[J]. *International Journal of Geomechanics*, 19(5):04019025.1-04019025.14.
- [2] FU Xiaodong, SHENG Qian, ZHANG Yonghui, et al, 2017. Time-Frequency Analysis of Seismic Wave Propagation across a Rock Mass Using the Discontinuous Deformation Analysis Method [J]. *International Journal of Geomechanics*, 2017:04017024.
- [3] ZHOU Xuefei, FAN Lifeng, WU Zhijun, 2017. Effects of Microfracture on Wave Propagation through Rock Mass [J]. *International journal of geomechanics*, 17(9):04017072.1-04017072.14.
- [4] FAN L.F., WANG L.J., WU Z.J., 2018. Wave transmission across linearly jointed complex rock masses[J]. *International Journal of Rock Mechanics and Mining ences*, 112:193-200.
- [5] GONG Wenjun, WANG Yunsheng, NING Youjun, et al, 2017. Validating the ability of the discontinuous deformation analysis method to model normal P-wave propagation across rock fractures[J]. *International Journal for Numerical & Analytical Methods in Geomechanics*, 41:1267–1282.
- [6] SHE Cheng-Xue, SUN Fu-Ting, 2017. Study of the Peak Shear Strength of a Cement-Filled Hard Rock Joint [J]. *Rock Mechanics and Rock Engineering*, 51:713–728.
- [7] MA Hao, LIU Quansheng, 2017. Prediction of the Peak Shear Strength of Sandstone and Mudstone Joints Infilled with High Water–Cement Ratio Grouts[J]. *Rock Mechanics and Rock Engineering*, 50:2021–2037.
- [8] LI Diyuan, HAN Zhenyu, ZHU Quanqi, et al, 2019. Stress wave propagation and dynamic behavior of red sandstone with single bonded planar joint at various angles[J]. *International Journal of Rock Mechanics & Mining Sciences*, 117:162-170.
- [9] HUANG Xiaolin, QI Shengwen, XIA Kaiwen, et al, 2018. Particle Crushing of a Filled Fracture During Compression and Its Effect on Stress Wave Propagation[J]. *Journal of Geophysical Research Solid Earth*, 123(7):5559-5587.